

# Evidence for Suppression of Collective Magnetism in Fe-Ag Granular Multilayers

László F. Kiss,\* László Bujdosó, and Dénes Kaptás

L.F. Kiss, L. Bujdosó, D. Kaptás  
Wigner Research Centre for Physics  
Budapest H-1525, P.O.Box 49, Hungary  
E-mail: kiss.laszlo.ferenc@wigner.hu

Keywords: dipolar interactions, magnetic anisotropy, magnetic nanoparticles, magnetic multilayers, memory effect, superparamagnetism, collective magnetism

## Abstract

Evidence for the suppression of collective magnetic behavior of dipolarly interacting Fe nanoparticles is found in Fe-Ag granular multilayers. Interaction of Fe particles located in neighboring Fe layers is studied as a function of the nominal thickness of the Ag layer in between only two Fe layers. The surprisingly increasing interaction with increasing Ag-layer thickness, verified by memory-effect measurements, is explained by the formation of pinholes in the Ag layer at small Ag thicknesses, allowing direct ferromagnetic coupling between Fe particles in neighboring Fe layers which may hinder the frustration of superspins favored by dipolar interactions. At larger Ag thicknesses, the Ag layer is continuous without pinholes and frustration leads to the appearance of the superspin-glass state. The effect of increasing interactions correlates well with the growing deviation at low temperatures of the measured field-cooled (FC) magnetization from the interaction-free FC curve calculated by a model based on the relaxation of two-level systems. Similar phenomenon is reported in a recently published paper (Sánchez et al., *Small* **2022**, 18, 2106762) where a dense nanoparticle system is studied. The collective magnetic behavior of the particles due to dipolar interactions is suppressed when the anisotropy energy of the individual particles exceeds a certain threshold.

## 1. Introduction

Fe-Ag multilayers containing few monolayers<sup>[1],[2]</sup> of Fe-layers show superparamagnetic (SPM) behavior of Fe islands. This is indicated by the linear temperature dependence of the magnetic hyperfine field<sup>[3]</sup> and the bifurcation of the magnetization of the field cooled (FC) and zero-field cooled (ZFC) sample.<sup>[4]</sup> The magnetic properties of such so-called

discontinuous or granular multilayers have been intensively studied,<sup>[5]</sup> similarly to granular alloys prepared by codeposition.<sup>[6], [7], [8]</sup> The SPM behavior depends not only on the magnetic anisotropy and the size distribution of the ferromagnetic particles but also on the strength of different type of (dipolar and/or exchange) intra- and interlayer interactions.<sup>[9], [10]</sup>

The general layer sequence of the Fe-Ag multilayer samples is Si/buffer +  $(t_{\text{Fe}} \text{ Fe} + t_{\text{Ag}} \text{ Ag})_n$  + cover where  $t_{\text{Fe}}$  and  $t_{\text{Ag}}$  are the nominal thicknesses of the Fe and Ag layers, respectively,  $n$  is the number of the Fe/Ag bilayers; “buffer” stands for a nonmagnetic metal layer evaporated directly on the smooth surface of the Si wafer (in our case it is Ag) and “cover” stands for a nonmagnetic layer which prevents the oxidation of the multilayer (here it is Nb).

The layer structure of some Fe-Ag multilayers was demonstrated by transmission electron microscopy.<sup>[11]</sup> Epitaxial bcc-Fe and fcc-Ag layers with a columnar-growth structure could be observed for  $t_{\text{Fe}} > 10 \text{ \AA}$  Fe but for a multilayer sample with smaller nominal Fe-layer thickness, neither Fe layers nor Fe nanoparticles could be identified. The determination of the average Fe-particle size from x-ray-diffraction line broadening<sup>[12]</sup> is hampered by the overlap of the diffraction lines of bcc Fe and fcc Ag while the (111) preferred orientation of the Ag layers could be observed.

In a previous paper,<sup>[13]</sup> we studied the magnetic properties of Fe-Ag multilayers fabricated with different  $t_{\text{Fe}}$ ,  $t_{\text{Ag}}$  and  $n$  parameters each covering a wide range. We found that below a certain value of  $t_{\text{Fe}}$ ,  $t_{\text{Ag}}$  and  $n$ , the Fe layers are discontinuous and these granular multilayers show the magnetic behavior of a superparamagnetic ensemble. Besides that increasing  $t_{\text{Fe}}$  increases the blocking temperature,  $t_{\text{Ag}}$  and  $n$  affect  $T_B$  not only by modifying the interactions between the Fe particles but also through influencing the growth process of Fe.

In a recent paper,<sup>[14]</sup> we investigated in detail the effect of interactions between the Fe particles on the SPM relaxation (ZFC and FC magnetization as a function of temperature, isotherm relaxation of magnetization as a function of time) in Fe-Ag multilayers containing a few bilayer numbers with constant  $t_{\text{Ag}}$  ( $t_{\text{Fe}} = 4\text{-}10 \text{ \AA}$ ,  $t_{\text{Ag}} = 50 \text{ \AA}$ ,  $n = 1, 10$ ). Increasing strength of dipolar interactions was evidenced with increasing  $t_{\text{Fe}}$  and  $n$ , probed by measuring the memory effect. We found an unambiguous correlation between the magnitude of the memory effect and the deviation of the low-field FC magnetization at low temperatures from the FC susceptibility curve of an interaction-free model of SPM particles.

Intensive research into the interactions between magnetic nanoparticles have been done in the last two-three decades.<sup>[9], [15]</sup> Kleemann et al. studied discontinuous  $\text{Co}_{80}\text{Fe}_{20}/\text{Al}_2\text{O}_3$  multilayers where the thickness of the magnetic layer separated by a non-magnetic and insulating spacer was varied. With increasing thickness, a transition sequence from superparamagnetic through super-spin glass (SSG) to superferromagnetic (SFM) behaviors could be observed.<sup>[16], [17], [18] [19], [20], [21], [22], [23], [24], [25], [26]</sup> Nordblad et al. explored the non-equilibrium dynamics in interacting magnetic nanoparticle systems, e.g.,  $\text{Fe-C}^{[27]}$  and  $\text{Fe}_3\text{N}^{[28]}$  and in systems showing similar phenomena such as spin glasses, e.g.,  $\text{CdCr}_{1.7}\text{In}_{0.3}\text{S}_4^{[29]}$   $\text{Ag(Mn)}^{[30], [31]}$  and  $\text{Cu(Mn)}^{[32]}$  While in these cases the cause of frustration leading to the SSG state was identified as dipolar interactions between the super-spins of the nanoparticles, other sources were also proved to induce this behavior. In magnetic Co-Ag granular films produced by cosputtering, a Ruderman-Kittel-Kasuya-Yosida- (RKKY) like exchange interaction between the nanoparticles was proposed to be responsible for the collective SSG dynamics.<sup>[33], [34]</sup> Similar mechanisms seem to be in action in  $\text{Cu}_{97.2}\text{Co}_{2.5}$  alloy prepared by melt spinning,<sup>[35]</sup>  $\text{Fe}_{30}\text{Ag}_{40}\text{W}_{30}$  fabricated by mechanical alloying<sup>[36]</sup> and annealed Cu-16Fe (at%) solid solutions obtained by high-pressure torsion.<sup>[37]</sup> The spin-glass phase of the outer shell of a very small nanoparticle with a core-shell structure may also influence the non-equilibrium dynamics of the particle ensemble.<sup>[38]</sup>

Mørup proposed<sup>[39]</sup> a phase diagram of dipolar-interacting magnetic-particle systems where the collective freezing temperature is determined exclusively by the strength of the dipolar interactions. However, the role of the individual particle anisotropy on influencing this temperature remained an open question. Very recently, Sánchez et al. studied<sup>[40]</sup> the influence of the individual particle anisotropy on the freezing temperature in a series of magnetic-particle assembly with similarly intense dipolar interactions but widely varying anisotropy. The anisotropy is tuned through different degrees of Co-doping in maghemite nanoparticles separated by each other by surfactants of different thicknesses. It was evidenced by experimental results and Monte Carlo simulations that the collective behavior (e.g., freezing temperature memory effect, ac susceptibility) depends on both the dipolar interactions and the anisotropy-energy barrier of the nanoparticles. Moreover, they suggest that the collective magnetic behavior is suppressed below a crossover value of  $T_{\text{MAX}}/T_{\text{B}} \approx 1.7$  (the ratio of the peak temperatures of the zero-field-cooled dc magnetization curves of dense and isolated systems made of the same nanoparticles) which corresponds to particle anisotropies above a

threshold of  $KV/E_{\text{dd}} \approx 130$  (the ratio of the anisotropy energy and dipolar interaction where  $K$  is the anisotropy constant and  $V$  is the particle volume).

In this paper, a Fe-Ag multilayer series was investigated containing two Fe layers with a nominal thickness of  $t_{\text{Fe}} = 4 \text{ \AA}$  separated by an Ag layer of nominal thicknesses of  $t_{\text{Ag}} = 8, 15, 26$  and  $50 \text{ \AA}$  ( $n = 2$ ) surrounded by buffer and cover layers. This series was fabricated in one evaporation run; therefore all layers of these samples except the varying Ag-layer separation were produced simultaneously under same circumstances. The aim of this investigation is to explore the interactions between the Fe particles located in the two neighboring Fe layers. As a result, it will turn out that the  $t_{\text{Ag}}$  dependence of the weak memory effect obtained cannot be interpreted solely by dipolar interactions but other factors (e.g., anisotropy) should be invoked, too, for the explanation.

In this paper, we use the stop-and-wait protocol as a genuine method to prove the existence of the SSG state of a nanoparticle system. The sample is cooled in zero field from above the blocking (freezing) temperature ( $T_{\text{B}}$ ) to a wait temperature,  $T_{\text{w}} < T_{\text{B}}$ , where it is kept for a wait time,  $t_{\text{w}}$ . Then the sample is cooled further to the lowest measuring temperature and the dc magnetization is measured upon warming, switching on a small magnetic field (called stop-and-wait curve). Repeating this procedure without stopping at  $T_{\text{w}}$ , a reference curve is measured and subtracting the latter from the former, a minimum close to  $T_{\text{w}}$  is obtained (called memory effect) but only if an SSG phase is present.<sup>[20], [21], [22], [23], [25], [26], [31], [34], [38]</sup> Besides the memory effect called this way because the sample showing a dip at  $T_{\text{w}}$  remembers on the annealing at  $T_{\text{w}}$  when it is reheated, a rejuvenation effect is also observed since after annealing at  $T_{\text{w}}$  and subsequent cooling, when reheating, the low-field dc magnetization returns to the reference curve and deviates from it only close to  $T_{\text{w}}$ . Both features are impossible in an interaction-free SPM nanoparticle ensemble.

## 2. Results

Figure 1 shows the ZFC and FC magnetizations for the multilayer series where two Fe layers each with  $t_{\text{Fe}} = 4 \text{ \AA}$  are surrounded by a Ag layer of varying thicknesses,  $t_{\text{Ag}} = 8, 15, 26$  and  $50 \text{ \AA}$ . For comparison, the results for the  $50 \text{ \AA Ag} + 4 \text{ \AA Fe} + 50 \text{ \AA Ag} + \text{cover}$  sample (with only one Fe layer) are also plotted.<sup>[14]</sup> The solid lines are fits to the theoretical model of interaction-free superparamagnetic particle ensemble using lognormal distributions for the activation energy ( $E = KV$ ) with median ( $E_{\text{m}}$ ) and width ( $\sigma$ ) parameters given in Table I. This model is

described in detail elsewhere;<sup>[14]</sup> however, a summary is given in the Experimental section of the present paper. The ZFC and FC magnetization vs. temperature curves shown in Figure 1 follow the typical behavior of a SPM assembly. The qualitative description of this behavior is well known. The magnetization of the sample cooled in zero field is small at low temperatures because the spatially random magnetic moments of the Fe particles (clusters) are frozen in during cooling through their respective blocking temperatures. The freezing occurs, depending on the time scale of the measurement, when the anisotropy energy of a cluster ( $KV$ ) exceeds the thermal energy ( $kT$ ). Upon warming in a magnetic field, the clusters gradually turn into the direction of the field when the thermal energy exceeds their respective anisotropy energies. Since the clusters have a size distribution, this results in a peak in the magnetization (ZFC curve). The temperature of the peak is called the average blocking temperature of the sample ( $T_B$ ). Above the highest individual blocking temperature of the clusters, the magnetization decreases like in a paramagnet. Upon cooling in magnetic field, the magnetic moments freeze aligned to the field, resulting in high magnetization at low temperatures. Upon warming in the same field, the FC curves are obtained (upper curves in Figure 1).

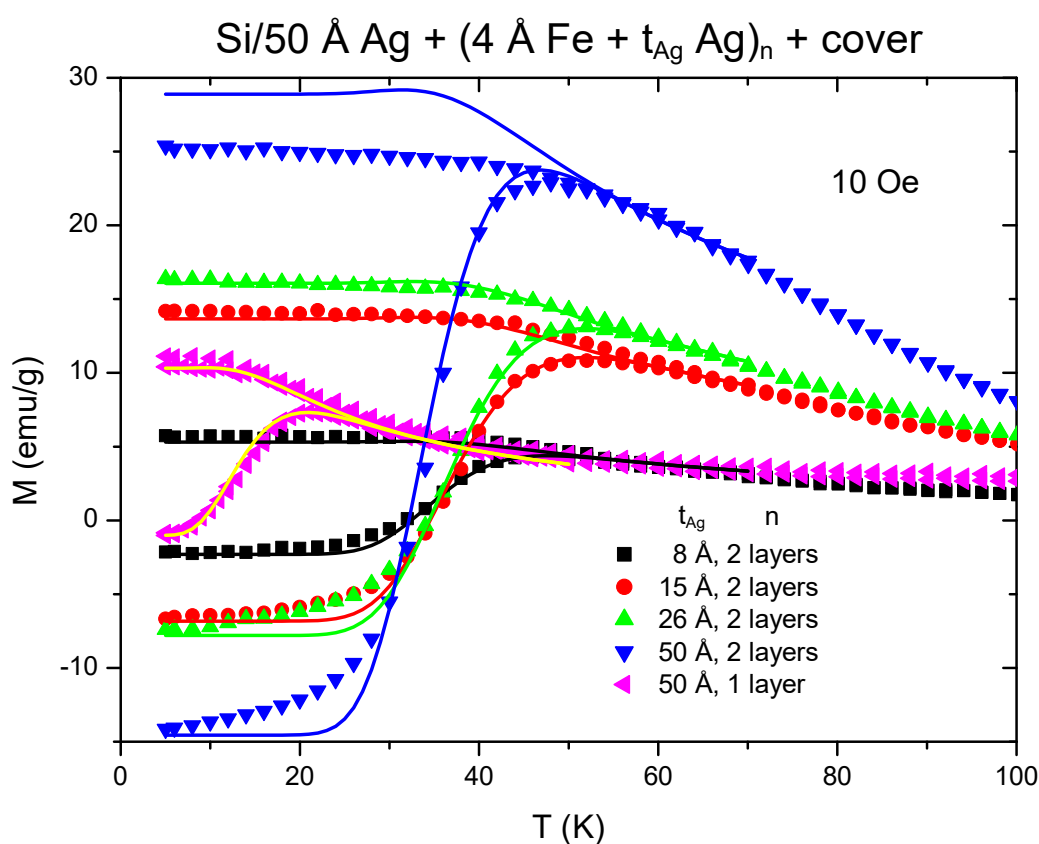


Figure 1. ZFC (lower curves) and FC (upper curves) magnetization as a function of temperature for the  $(4 \text{ \AA Fe} + t_{\text{Ag}} \text{ Ag})_2 + \text{cover}$  sample series ( $t_{\text{Ag}} = 8, 15, 26$  and  $50 \text{ \AA}$ ). For comparison, the curves for the  $50 \text{ \AA Ag} + 4 \text{ \AA Fe} + 50 \text{ \AA Ag} + \text{cover}$  sample are also plotted.<sup>[14]</sup> The measuring field is  $H = 10 \text{ Oe}$ . The solid lines are fits to the theoretical model of interaction-free superparamagnetic particle ensemble (see Experimental section) using lognormal distributions for the activation energy ( $E = KV$ ) with median ( $E_m$ ) and width ( $\sigma$ ) parameters given in Table I. The small negative remanent field of the superconducting coil and the consequent negative magnetization values at low temperatures are taken into account with a slightly asymmetric initial population of the energy levels of the two-level systems (TLS), i.e.,  $n_0 > 0.5$  (see details in Experimental Section and Ref.[14]).

$t_{\text{Ag}} (\text{\AA})$	8	15	26	50
$E_m (\text{eV})$	0.084	0.089	0.089	0.082
$\sigma (\text{eV})$	0.16	0.18	0.18	0.16
$T_B (\text{K})$	46	51	52	47
$T_B/T_B^*$	2.19	2.43	2.48	2.24

Table 1 Activation-energy median ( $E_m$ ) and width ( $\sigma$ ) of the lognormal distribution (see Experimental Section for definition) used for fitting the ZFC and FC magnetization vs. temperature curves of the  $(4 \text{ \AA Fe} + t_{\text{Ag}} \text{ Ag})_2 + \text{cover}$  sample series shown in Figure 1 to the theoretical interaction-free model of superparamagnetic particle ensemble.  $T_B$  is the blocking temperature (peak temperature of the ZFC curve).  $T_B^* = 21 \text{ K}$  is  $T_B$  of the  $50 \text{ \AA Ag} + 4 \text{ \AA Fe} + 50 \text{ \AA Ag} + \text{cover}$  sample regarded as the reference system without interaction.<sup>[14]</sup>

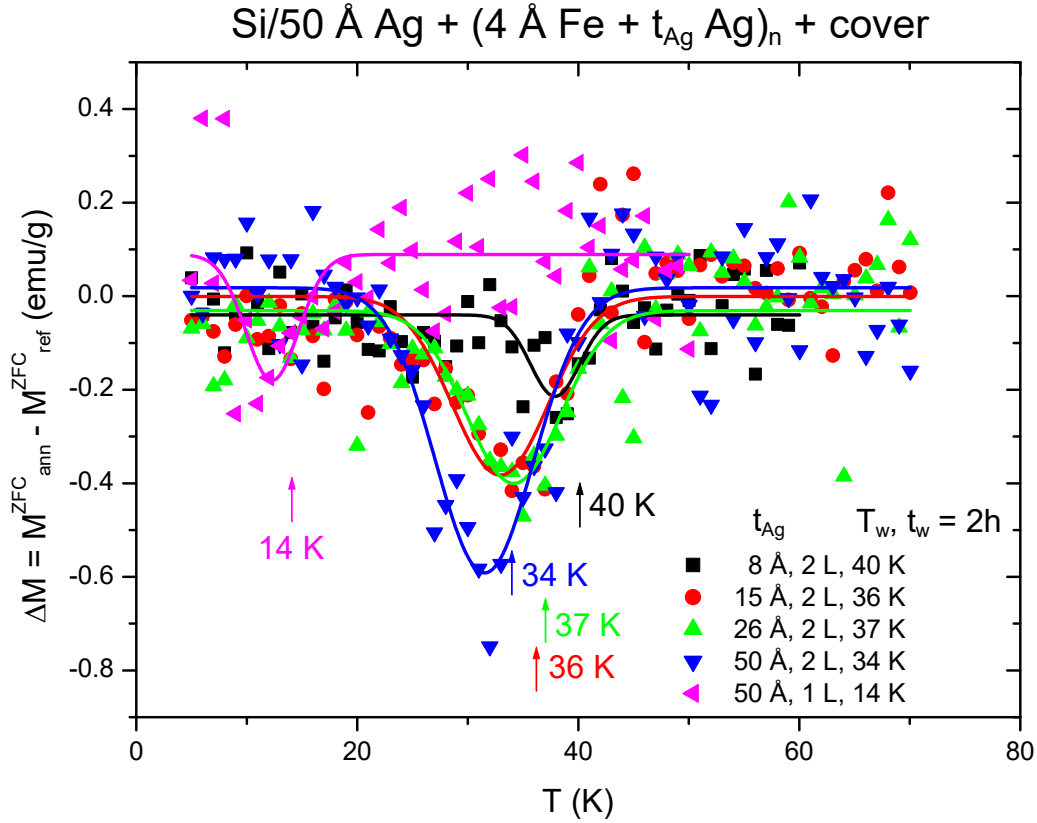


Figure 2 Memory effect for the  $(4\text{Å Fe} + t_{\text{Ag}}\text{ Ag})_2 + \text{cover}$  sample series ( $t_{\text{Ag}} = 8, 15, 26$  and  $50\text{ Å}$ ) with wait time,  $t_w = 2\text{h}$ , and wait temperatures,  $T_w$ , indicated in the figure. For comparison, the curve for the  $50\text{ Å Ag} + 4\text{ Å Fe} + 50\text{ Å Ag} + \text{cover}$  sample is also plotted.<sup>[14]</sup> The ZFC magnetization both in the annealed and the reference states as a function of temperature was measured in  $H = 10\text{ Oe}$ . The arrows and temperatures denoted by labels show the wait temperatures,  $T_w$ , where the respective sample was annealed for  $t_w = 2\text{h}$ . L means layer and the lines are Gauss fits used as guides to the eye.

As seen in Figure 1, the blocking temperature is doubled when the bilayer number is increased from  $n = 1$  to 2 for the sample with  $t_{\text{Fe}} = 4\text{ Å}$  and  $t_{\text{Ag}} = 50\text{ Å}$ . This behavior is in line with the trend found previously<sup>[13]</sup> and can be explained by the changing morphology during the columnar-structure growth of the layers preferring larger cluster sizes with increasing  $n$ . However, decreasing the Ag-layer thickness from  $t_{\text{Ag}} = 50$  to  $8\text{ Å}$ ,  $T_B$  remains practically constant. This result is surprising for two reasons: (i) we obtained previously<sup>[13]</sup> that  $T_B$  increases with decreasing  $t_{\text{Ag}}$  for a multilayer series with  $t_{\text{Fe}} = 2\text{ Å}$  and  $n = 75$ ; and (ii) the dipolar interactions between the Fe clusters in the adjacent two layers are expected to increase

with decreasing  $t_{\text{Ag}}$ , resulting in a higher  $T_{\text{B}}$ . The measured  $T_{\text{B}}$  values can be regarded reliable since this sample series was fabricated in one evaporation cycle.

Figure 2 shows the memory effect for the same samples as in Figure 1 with wait time,  $t_{\text{w}} = 2\text{h}$ , and wait temperatures,  $T_{\text{w}}$ , indicated in the figure. The memory effect is almost absent for the  $t_{\text{Ag}} = 8 \text{ \AA}$  sample with two Fe layers ( $t_{\text{Fe}} = 4 \text{ \AA}$ ,  $n = 1$ ) and also for the  $4 \text{ \AA Fe} + 50 \text{ \AA Ag}$  sample containing a single Fe layer. Though a tiny dip close to  $T_{\text{w}}$  can be surmised for both samples as shown by the Gauss fits (used as guides to the eye), the presence of memory effect cannot be unambiguously stated because of the large scattering of the measuring points. The memory effect is very small but clearly observable for  $t_{\text{Ag}} = 15$  and  $26 \text{ \AA}$  and it is definitely larger for  $t_{\text{Ag}} = 50 \text{ \AA}$  of the sample series consisting of two Fe layers.

Similarly as found for the  $50 \text{ \AA Ag} + t_{\text{Fe}} \text{ Fe} + 50 \text{ \AA Ag} + \text{cover}$  sample series with a single Fe layer having nominal thicknesses of  $t_{\text{Fe}} = 4, 5, 7$  and  $10 \text{ \AA}$ ,<sup>[14]</sup> a correlation is observed in Figures 1 and 2 between the behavior of the FC magnetization and the memory effect for the presently studied  $(4 \text{ \AA Fe} + t_{\text{Ag}} \text{ Ag})_2 + \text{cover}$  sample series ( $t_{\text{Ag}} = 8, 15, 26$  and  $50 \text{ \AA}$ ). In these two-Fe-layer sample series, there is a systematic deviation of the theoretical FC curve from the measured one below  $T_{\text{B}}$  for larger  $t_{\text{Ag}}$  while the theoretical ZFC curves describe relatively well the measured ones for all  $t_{\text{Ag}}$ . For larger  $t_{\text{Ag}}$ , the measured FC magnetization remains below the calculated curve (for  $t_{\text{Ag}} = 50 \text{ \AA}$  significantly), becoming more and more flattened without exhibiting any plateau at low temperatures. The correlation found between the appearance of the memory effect and the flattening of the FC magnetization curve was previously attributed to the appearance of dipolar interactions between the Fe clusters.<sup>[14]</sup> Similar observations were reported by Binns et al.<sup>[7]</sup> and Denardin et al.<sup>[41]</sup> The rising of the theoretical FC curve at low temperatures is a consequence of the non-collective behavior of the clusters, causing the freezing of the individual magnetic moments upon cooling, independently from each other, aligned to the direction of the field. The comparison of the measured and theoretical FC magnetization curves leads to the conclusion that the multilayer sample with  $t_{\text{Ag}} = 8 \text{ \AA}$  can be well described by the interaction-free model. Increasing  $t_{\text{Ag}}$ , the interactions should increase as is obvious from the increasing deviation between the measured and model FC curves at low temperatures (Figure 1). This surprising trend is corroborated by the results of the memory-effect measurements (Figure 2) proving that the interlayer interactions should increase with increasing  $t_{\text{Ag}}$ .

It is obvious that the increasing memory effect with increasing  $t_{\text{Ag}}$  cannot be explained exclusively by the dipolar interactions between the Fe clusters. There must be another effect in play which counteracts the tendency of the dipolar interactions to frustrate the magnetic moments at small  $t_{\text{Ag}}$ .

### 3. Discussion

For the multilayer series with two nominal Fe layers,  $(4 \text{ \AA Fe} + t_{\text{Ag}} \text{ Ag})_2 + \text{cover}$  ( $t_{\text{Ag}} = 8, 15, 26$  and  $50 \text{ \AA}$ ), a surprising result is obtained for the  $t_{\text{Ag}}$  dependence of the memory effect (Figure 2), supported also by the behavior of the low-field FC magnetization at low temperatures (Figure 1): the memory effect, i.e., the interactions between the clusters increase with increasing Ag-layer thickness. Since the presence of dipolar interactions only would cause an opposite dependence, we have to assume other factors, too, influencing the possibility of the superspins to become frustrated, i.e., to form an SSG state.

Besides the dipolar interaction, it is the RKKY exchange interaction which might cause an SSG state of the superspins in granular alloys in which the magnetic particles are separated by a non-magnetic metallic (conductive) matrix.<sup>[33], [34], [35], [36], [37]</sup> In these cases, a small part of Co is dissolved in Ag<sup>[33], [34]</sup> and Cu<sup>[35]</sup> matrix or a small part of Fe in Cu matrix<sup>[37]</sup> where the dissolved magnetic atoms or groups containing a few of them strengthen the effect of the RKKY interaction between the magnetic particles. It is obvious that this mechanism could not work in Fe/Ag systems since the solubility of Fe in Ag is very small compared to the previous cases. Intermixing of Fe and Ag could be verified only in two-monolayer thickness at the interface between Fe and Ag layers of a Ag/Fe/Ag trilayer with the help of magnetoresistance measurements.<sup>[42]</sup> Moreover, the RKKY interaction would lead to an opposite dependence of the memory effect with increasing Ag-layer thickness as was observed for our  $(4 \text{ \AA Fe} + t_{\text{Ag}} \text{ Ag})_2 + \text{cover}$  ( $t_{\text{Ag}} = 8, 15, 26$  and  $50 \text{ \AA}$ ) multilayer series (Figure 1). Since the RKKY interaction significantly weakens with increasing  $t_{\text{Ag}}$  in the studied  $t_{\text{Ag}}$  range, the memory effect should decrease with increasing  $t_{\text{Ag}}$ , were it caused by this interaction.

Despite all of this, an oscillatory RKKY indirect exchange coupling of ferromagnetic layers (e.g., Co) via non-magnetic spacer layers (e.g., Cu) exists and is verified in multilayers even with contiguous (not granular) layer structure.<sup>[43]</sup> This oscillating coupling, i.e., alternating ferromagnetic (FM) and antiferromagnetic (AFM) interlayer interaction as a function of the thickness of the non-magnetic spacer layer, can be demonstrated by magnetoresistance

measurements but magnetization studies often fail to prove the existence of AFM couplings.<sup>[44], [45]</sup> It was shown that structural imperfections (e.g., pinholes) in the spacer layers give rise to direct FM coupling of neighboring ferromagnetic layers.

The discontinuity of an Ag layer below a thickness of 50 Å was shown by Mössbauer spectroscopy in B/Fe/Ag multilayer samples.<sup>[46]</sup> The blocking temperature of one nominally 4-Å thick Fe granular layer evaporated on an Ag layer of varying thicknesses shows a minimum at  $t_{\text{Ag}} = 40\text{-}70$  Å which was also explained by the onset of such discontinuities called pinholes below a critical thickness at  $t_{\text{Ag}} \sim 50$  Å.<sup>[13]</sup> This observation offers a plausible interpretation for the anomalous behavior of the Ag-thickness dependence of the memory effect in the  $(4 \text{ Å Fe} + t_{\text{Ag}} \text{ Ag})_2 + \text{cover}$  ( $t_{\text{Ag}} = 8, 15, 26$  and  $50$  Å) multilayer series (Figure 2). At small  $t_{\text{Ag}}$ , the Fe particles located in the neighboring Fe layers become FM coupled via pinholes in the Ag layer separating them, hindering the frustration of the superspins, hence the appearance of the SSG state. With increasing  $t_{\text{Ag}}$ , this effect gradually ceases as the Ag layer becomes contiguous, and the dipolar interactions between the Fe clusters (or at least between parts of them) are able to form an SSG state evidenced by the memory effect measured. The RKKY interaction would not be effective at Ag thicknesses close to  $t_{\text{Ag}} = 50$  Å. The observation that the blocking temperature does not vary with  $t_{\text{Ag}}$  in this multilayer series (Figure 1) might be the consequence of a delicate balance of both effects. At small  $t_{\text{Ag}}$ ,  $T_{\text{B}}$  is increased with respect to the one-Fe-layer case ( $n = 1$ ) because of the direct contact of Fe particles via pinholes resulting in larger average particle volume while at larger  $t_{\text{Ag}}$  in absence of this effect, the  $T_{\text{B}}$  increase is caused by the dipolar interactions, apparently increasing the average particle volume. The previously obtained increasing  $T_{\text{B}}$  with decreasing  $t_{\text{Ag}}$  in the same  $t_{\text{Ag}}$  range for the  $t_{\text{Fe}} = 2$  Å and  $n = 75$  multilayer series<sup>[13]</sup> apparently contradicts the above observed finding. However, we found evidence in the same paper for the increase of the Fe-particle size along the multilayer stack as the subsequent layers are evaporated. The significant  $T_{\text{B}}$  increase with increasing bilayer number measured in Fe-Ag multilayers<sup>[13]</sup> was partly explained by this particle-size increase. We think this is the reason for the different behavior of the  $T_{\text{B}}$  vs.  $t_{\text{Ag}}$  dependence when the bilayer number is increased from  $n = 2$  to 75.

For the  $(26 \text{ Å Ag} + t_{\text{Fe}} \text{ Fe})_{10}$  multilayer series ( $2 \text{ Å} \leq t_{\text{Fe}} \leq 10 \text{ Å}$ ), a change in the direction of the spontaneous magnetization from out-of-plane to in-plane was observed with increasing  $t_{\text{Fe}}$  at  $t_{\text{Fe}} \sim 6$  Å by Mössbauer spectroscopy.<sup>[47]</sup> Since the appearance of perpendicular anisotropy below  $t_{\text{Fe}} \sim 6$  Å seems to be an intrinsic property of Fe-Ag multilayers, an out-of-plane

anisotropy can be assumed also for the  $(4 \text{ \AA Fe} + t_{\text{Ag}} \text{ Ag})_2 + \text{cover}$  ( $t_{\text{Ag}} = 8, 15, 26$  and  $50 \text{ \AA}$ ) multilayer series studied here. We think that at small  $t_{\text{Ag}}$ , the perpendicular anisotropy might strengthen the effect of pinholes in hindering the frustration of the superspins.

The mechanism which we used to explain the suppression of collective magnetic behavior for decreasing thickness of the Ag-layer surrounded by two Fe layers in the studied Fe-Ag granular multilayer series is very similar to the interpretation of Sánchez et al.<sup>[40]</sup> In their nanoparticle system, the particle volumes are almost constant (with narrow particle-size distribution) and the anisotropy constant is increased by nearly an order of magnitude with Co-doping. In our case, the anisotropy constant does not vary significantly but the particle volumes should increase by contacts through pinholes for decreasing  $t_{\text{Ag}}$ . In both cases, the anisotropy energy ( $KV$ ) increases, leading to the suppression of collective magnetism. In our case, the  $50 \text{ \AA Ag} + 4 \text{ \AA Fe} + 50 \text{ \AA Ag} + \text{cover}$  sample containing only one Fe layer can be regarded as the reference sample without interaction. The ratio of the peak temperatures of the ZFC magnetization curves of the two-Fe-layer samples and the one-Fe-layer reference sample,  $T_B/T_B^*$  (which corresponds to  $T_{\text{MAX}}/T_B$  in Ref.[40]) varies between 2.19 and 2.48 (Table 1). These values are somewhat larger than the threshold of 1.7 found by Sánchez et al.<sup>[40]</sup> The reason for this difference might be that the nanoparticle system in the Fe-Ag granular multilayers is not as ideal as that studied in Ref.[40]. As it was pointed out in a previous paper,<sup>[13]</sup> the increase of  $T_B$  with increasing bilayer number in Fe-Ag granular multilayers is partly related to the increase of the particle size in successive Fe layers during the evaporation process. Therefore, the particle volumes are not monodisperse; instead, the particle size can almost be doubled in the second Fe layer with respect to the first one. Broader particle-size distributions require higher ratios of  $T_B/T_B^*$  to reach collective behavior.<sup>[40]</sup>

The measurement of the ZFC and FC magnetization curves of a dense nanoparticle system, fitted with the help of the proposed model of an interaction-free SPM particle assembly is an easy experimental method to assess the collective character of magnetic behavior of the system. It is even easier than the method proposed by Sánchez et al.<sup>[40]</sup> because in our case no interaction-free reference system is needed for the prediction.

#### 4. Conclusions

Superparamagnetic Fe-Ag granular multilayers where the nominal thickness of a Ag layer located between two nominally 4-Å thick Fe layers is increased from  $t_{\text{Ag}} = 8$  to 50 Å were investigated by measuring the ZFC and FC magnetization curves and the memory effect with the help of the stop-and-wait protocol. For increasing  $t_{\text{Ag}}$ , an increase of the memory effect was observed despite the decreasing dipolar interactions. We found an unambiguous correlation between the magnitude of the memory effect and the deviation of the low-field FC magnetization at low temperatures from the FC susceptibility curve of an interaction-free model of SPM particles. The suppression of collective magnetic behavior for decreasing  $t_{\text{Ag}}$  is explained by the formation of pinholes in the Ag layer at small thicknesses, bringing about ferromagnetic coupling between the Fe particles in adjacent Fe layers, which may impede the frustration of the superspins.

## 5. Experimental Section

The multilayer samples were fabricated by vacuum evaporation. The detailed description of the equipment can be found elsewhere.<sup>[13],[14]</sup> We stress only that the two substrate holders and an appropriate shutter enable the preparation of two (in some cases four) samples with fully or partially identical layer structure.

The magnetization of the samples was measured using a MPMS-5S Quantum Design superconducting interference device (SQUID) between 5 and 300 K and 0 and 50 kOe. The low-field measurements were performed in  $H = 10$  Oe upon warming after cooling the samples from 300 to 5 K in zero field (ZFC) or in the measuring field of  $H = 10$  Oe (FC). Because of the remanent field of the superconducting magnet, the minimum field that can be reached by this procedure is around  $-1$  Oe. Therefore, the magnetization of the ZFC vs. temperature curves shown in this paper assumes negative values. Such an effect has been reported in the literature.<sup>[48],[49]</sup> One or two pieces of  $\sim 6 \times 6$ -mm<sup>2</sup> Si wafer were pressed between the walls of a drinking straw without using any sample-supporting part. In case of two pieces, they were stacked with the multilayer of each on the surface. The memory effect is obtained by measuring the low-field dc magnetization using the stop-and-wait protocol described in detail in the Introduction. The wait temperatures,  $T_w$ , are selected to be around the inflexion point of the ZFC magnetization curve where considerable relaxation can be expected. The presented memory-effect curves vs. temperature have similar  $T_w/T_B$  ratio (between 0.7-0.85) for the sake of quantitative comparability.

The measured ZFC and FC magnetization curves were compared with those of a theoretical model of superparamagnetic particle ensemble without interaction. The model is based on the fact that from energetic point of view an ensemble of single-domain particles can be described by an ensemble of two-level systems (TLS).<sup>[50]</sup> The two minima correspond to the two stable or metastable directions of the magnetic moments between which transitions can occur by thermal excitation. In zero field, the TLSs are symmetric with an energy barrier of  $E_a = KV$  where  $K$  is the anisotropy constant and  $V$  is the volume of the particles.  $K$  is assumed to be constant while the distribution of  $V$  is approximated by a lognormal distribution

$$p(E_a) = \frac{1}{\sqrt{2\pi\sigma E_a}} \exp \left[ -\frac{1}{2} \left( \frac{\ln \frac{E_a}{E_m}}{\sigma} \right)^2 \right]$$

where  $E_a = KV$  is the anisotropy energy,  $E_m$  is the median and  $\sigma$  is the width of the distribution. Applying a small magnetic field makes the TLSs asymmetric, characterized by activation-energy and splitting parameters. The small negative remanent field of the superconducting coil and the consequent negative magnetization values at low temperatures are taken into account with a slightly asymmetric initial population of the energy levels of the TLSs, i.e.,  $n_0 > 0.5$ . The detailed description of the model can be found elsewhere.<sup>[14]</sup>

## Acknowledgements

The Wigner Research Centre for Physics utilizes the research infrastructure of the Hungarian Academy of Sciences and is operated by the Eötvös Loránd Research Network (ELKH) Secretariat (Hungary). Financial support by the Hungarian Scientific Research Fund (Grant No. OTKA-K-112811) is greatly acknowledged.

- 
- [1] N.C. Koon, B.T. Jonker, F.A. Volkening, J.J. Krebs, G.A. Prinz, *Phys. Rev. Lett.* **1987**, 59, 2463.  
[2] F.A. Volkening, B.T. Jonker, J.J. Krebs, N.C. Koon, G.A. Prinz, *J. Appl. Phys.* **1988**, 63, 3869.  
[3] Z.Q. Qiu, S.H. Mayer, C.J. Gutierrez, H. Tang, J.C. Walker, *Phys. Rev. Lett.* **1989**, 63, 1649.  
[4] J. Balogh, D. Kaptás, L.F. Kiss, L. Pusztai, E. Szilágyi, Á. Tunyogi, J. Swerts, S. Vandezande, K. Temst, C. Van Haesendonck, *Appl. Phys. Lett.* **2005**, 87, 102501.  
[5] J. Balogh, D. Kaptás, I. Vincze, K. Temst, C. Van Haesendonck, *Phys. Rev. B* **2007**, 76, 052408.  
[6] M.A. Arranz, J.P. Andrés, J.A. De Toro, S.E. Paje, M.A. López de la Torre, J.M. Riveiro, *J. Magn. Magn. Mater.* **2002**, 242-245, 952.  
[7] C. Binns, M.J. Maher, Q.A. Pankhurst, D. Kechrakos, K.N. Trohidou, *Phys. Rev. B* **2002**, 66, 184413.  
[8] C. Binns, K.N. Trohidou, J. Bansmann, S.H. Baker, J.A. Blackman, J.-P. Bucher, D. Kechrakos, A. Kleibert, S. Louch, K.-H. Meiwes-Broer, G.M. Pastor, A. Perez, Y. Xie, *J. Phys. D* **2005**, 38, R357.  
[9] J.L. Dormann, D. Fiorani, E. Tronc, in *Advances in Chemical Physics*, edited by I. Prigogine and S. Rice (Wiley, New York, **1997**), Vol. 68, p. 283, and references therein.  
[10] M. Knobel, W.C. Nunes, L.M. Socolovsky, E. De Biasi, J.M. Vargas, J.C. Denardin, *J. Nanosci. Nanotechn.* **2008**, 8, 2836.  
[11] M. Csontos, J. Balogh, D. Kaptás, L.F. Kiss, A. Kovács, G. Mihály, *Phys. Rev. B* **2006**, 73, 184412.

- 
- [12] J. Balogh, D. Kaptás, T. Kemény, L.F. Kiss, T. Pusztai, I. Vincze, *Hyperfine Interactions* **2002**, 141-142, 13.
- [13] L.F. Kiss, J. Balogh, L. Bujdosó, D. Kaptás, *Phys. Rev. B* **2018**, 98, 144423.
- [14] L.F. Kiss, J. Balogh, L. Bujdosó, D. Kaptás, *Mater. Res. Express* **2021**, 8, 106101.
- [15] S. Bedanta, W. Kleemann, *J. Phys. D: Appl. Phys.* **2009**, 42, 013001.
- [16] W. Kleemann, Ch. Binek, O. Petravic, G.N. Kakazei, Yu.G. Pogorelov, J.B. Sousa, M.M Pereira de Azevedo, S. Cardoso, P.P. Freitas, *J. Magn. Magn. Mater.* **2001**, 226-230, 1825.
- [17] W. Kleemann, O. Petravic, Ch. Binek, G.N. Kakazei, Yu.G. Pogorelov, J.B. Sousa, S. Cardoso, P.P. Freitas, *Phys. Rev. B* **2001**, 63, 134423.
- [18] S. Sahoo, O. Petravic, Ch. Binek, W. Kleemann, J.B. Sousa, S. Cardoso, P.P. Freitas, *Phys. Rev. B* **2002**, 65, 134406.
- [19] S. Sahoo, O. Petravic, Ch. Binek, W. Kleemann, J.B. Sousa, S. Cardoso, P.P. Freitas, *J. Phys.: Condens. Matter* **2002**, 14, 6729.
- [20] S. Sahoo, O. Petravic, W. Kleemann, S. Stappert, G. Dumpich, P. Nordblad, S. Cardoso, P.P. Freitas, *Appl. Phys. Lett.* **2003**, 82, 4116.
- [21] S. Sahoo, O. Petravic, W. Kleemann, P. Nordblad, S. Cardoso, P.P. Freitas, *Phys. Rev. B* **2003**, 67, 214422.
- [22] S. Bedanta, X. Chen, S. Sahoo, W. Kleemann, E. Kentzinger, P. Nordblad, S. Cardoso, P.P. Freitas, *Phys. Stat. Sol. (c)* **2004**, 1, 3288.
- [23] S. Sahoo, O. Petravic, W. Kleemann, P. Nordblad, S. Cardoso, P.P. Freitas, *J. Magn. Magn. Mater.* **2004**, 272-276, 1316.
- [24] Xi. Chen, S. Sahoo, W. Kleemann, S. Cardoso, P.P. Freitas, *Phys. Rev. B* **2004**, 70, 172411.
- [25] Xi. Chen, S. Bedanta, O. Petravic, W. Kleemann, S. Sahoo, S. Cardoso, P.P. Freitas, *Phys. Rev. B* **2005**, 72, 214436.
- [26] O. Petravic, X. Chen, S. Bedanta, W. Kleemann, S. Sahoo, S. Cardoso, P.P. Freitas, *J. Magn. Magn. Mater.* **2006**, 300, 192.
- [27] P. Jönsson, M.F. Hansen, P. Nordblad, *Phys. Rev. B* **2000**, 61, 1261.
- [28] M. Sasaki, P.E. Jönsson, H. Takayama, H. Mamiya, *Phys. Rev. B* **2005**, 71, 104405.
- [29] K. Jonason, E. Vincent, J. Hamman, J.P. Bouchaud, P. Nordblad, *Phys. Rev. Lett.* **1998**, 81, 3243.
- [30] T. Jonsson, K. Jonason, P. Jönsson, P. Nordblad, *Phys. Rev. B* **1999**, 59, 8770.
- [31] R. Mathieu, P. Jönsson, D.N.H. Nam, P. Nordblad, *Phys. Rev. B* **2001**, 63, 092401.
- [32] C. Djurberg, K. Jonason, P. Nordblad, *Eur. Phys. J. B* **1999**, 10, 15.
- [33] J.A. De Toro, J.P. Andrés, J.A. González, J.P. Goff, A.J. Barbero, J.M. Riveiro, *Phys. Rev. B* **2004**, 70, 224412.
- [34] J. Du, B. Zhang, R.K. Zheng, X.X. Zhang, *Phys. Rev. B* **2007**, 75, 014415.
- [35] A. López, F.J. Lázaro, M. Artigas, A. Larrea, *Phys. Rev. B* **2002**, 66, 174413.
- [36] J.A. De Toro, M.A. López de la Torre, J.M. Riveiro, A. Beesley, J.P. Goff, M.F. Thomas, *Phys. Rev. B* **2004**, 69, 224407.
- [37] M. Stückler, H. Krenn, P. Kürnsteiner, B. Gault, F. De Geuser, L. Weissitsch, S. Wurster, R. Pippan, A. Bachmaier, *Acta Mater.* **2020**, 196, 210.
- [38] B. Zhang, J. Gao, B. Xu, X.X. Zhang, *Eur. Phys. Lett.* **2010**, 91, 57006.
- [39] S. Mørup, *Eur. Phys. Lett.* **1994**, 28, 671.
- [40] E.H. Sánchez, M. Vasilakaki, S.S. Lee, P.S. Normile, M.S. Andersson, R. Mathieu, A. López-Ortega, B.P. Pichon, D. Peddis, C. Binns, P. Nordblad, K. Trohidou, J. Nogués, J.A. De Toro, *Small* **2022**, 18, 2106762.
- [41] J.C. Denardin, A.L. Brandl, M. Knobel, P. Panissod, A.B. Pakhomov, H. Liu, X.X. Zhang, *Phys. Rev. B* **2002**, 65, 064422.
- [42] J. Balogh, L.F. Kiss, A. Halbritter, I. Kézsmárki, G. Mihály, *Solid State Commun.* **2002**, 122, 59.
- [43] S.S.P. Parkin, R. Bhadra, K.P. Roche, *Phys. Rev. Lett.* **1991**, 66, 2152
- [44] S.S.P. Parkin, R.F. Marks, R.F.C. Farrow, G.R. Harp, Q.H. Lam, R.J. Savoy, *Phys. Rev. B* **1992**, 46, 9262.
- [45] J.W. Freeland, D.J. Keavney, D.F. Storm, I.L. Grigorov, J.C. Walker, M.G. Pini, P. Politi, A. Rettori, *Phys. Rev. B* **1996**, 54, 9942.
- [46] J. Balogh, L. Bujdosó, D. Kaptás, I. Dézsi, A. Nakanishi, *Phys. Rev. B* **2012**, 85, 195429.
- [47] J. Balogh, Cs. Fetzer, D. Kaptás, L.F. Kiss, I.S. Szűcs, I. Dézsi, I. Vincze, *Phys. Status Solidi* **2008**, 205, 1828.
- [48] V. Stanciu, I.L. Soroka, J. Lu, B. Hjörvarsson, P. Nordblad, *J. Magn. Magn. Mater.* **2005**, 286, 446.
- [49] P.T. Korelis, P.E. Jönsson, A. Liebig, H.-E. Wannberg, P. Nordblad, B. Hjörvarsson, *Phys. Rev. B* **2012**, 85, 214430.
- [50] B.D. Cullity, C.D. Graham, *Introduction to Magnetic Materials*, John Wiley and Sons, Hoboken **2009**, p. 315.